

Sensor and Simulation Notes

Note 385

November 1995

Feed-Point Lenses for Half Reflector IRAs

**Everett G. Farr
Farr Research**

**Carl E. Baum
Phillips Laboratory**

Abstract

A critical component of a high-voltage Half Impulse Radiating Antenna (HIRA) is the lens, which is located at the feed point. This lens is used to match an electrically large coaxial waveguide to the feed arms of a Half IRA. It consists of a prolate spheroidal surface at one interface, and a quartic surface on the other interface. We describe here the design principles of this lens, and we provide example solutions.

NOTED
FOR PUBLIC RELEASE

PA/PI 12-19-95

PL 95 - 100.1

I. Introduction

The availability of single-ended high-voltage pulsers has led to the demand for suitable antennas to radiate the signal. A candidate antenna for this application is the Half Impulse Radiating Antenna (HIRA). This antenna was first proposed in [1], and a variation of this was described in [2].

Probably the most complicated part of this antenna design is the lens. This lens is used to convert a plane wave in a coaxial waveguide to a spherical wave which is launched onto the conical feed arms. Normally, one would want to keep this region electrically small, but high voltages preclude that possibility. An idealized version of the lens was proposed in [3], but this version required a material whose dielectric constant could be varied continuously throughout the medium. This design also required guiding conductors spaced close together, on sheets of constant theta, to guide the waves. In this paper we propose a lens that is built with a simple homogeneous dielectric material, so it will be more practical to build.

An example of a typical HIRA is sketched in Figure 1.1. It consists of an oil-filled coaxial feed, which transitions into the feed arms of the antenna. The antenna itself consists of two conical feed arms feeding half a reflector. We assume an F/D ratio of 0.25, in order to maintain rotational symmetry. The input impedance to the feed arms is typically 100Ω in air, or about 67Ω in the oil-filled coaxial feed. This particular sketch includes an oil cap above the ground plane, but other designs are available without the oil cap. The outer edge of the oil cap is a spherical polyethylene shell, which has a dielectric constant close to oil, so it does not change the direction of the field.

For the purposes of our calculations, we assume a lens feed and antenna with a single conical arm. Normally, one will want to split the center conductor into two arms, but we can only solve the problem if it is rotationally symmetric. The solution to the rotationally symmetric case provides a good approximation to the more difficult three-dimensional problem.

Sketches of two possible lens designs are shown in Figure 1.2. The first sketch shows a design which includes an oil cap. We will refer to this as an oil-lens-oil design. The second design has no oil cap and it simply has air or SF_6 at its output. We refer to this design as the oil-lens-air design. The equations for both designs are quite similar, and we provide equations general enough to include both.

The net effect of the lens is to convert a plane wave in a coaxial geometry to a spherical wave in a conical geometry. The focus of the spherical wave is on the ground plane, at the center of the coaxial feed, and at the focus of the paraboloid.

In this paper we provide a complete derivation of the lens equations. We also provide design principles, and we show some examples. Let us begin now with derivations of the lens equations.

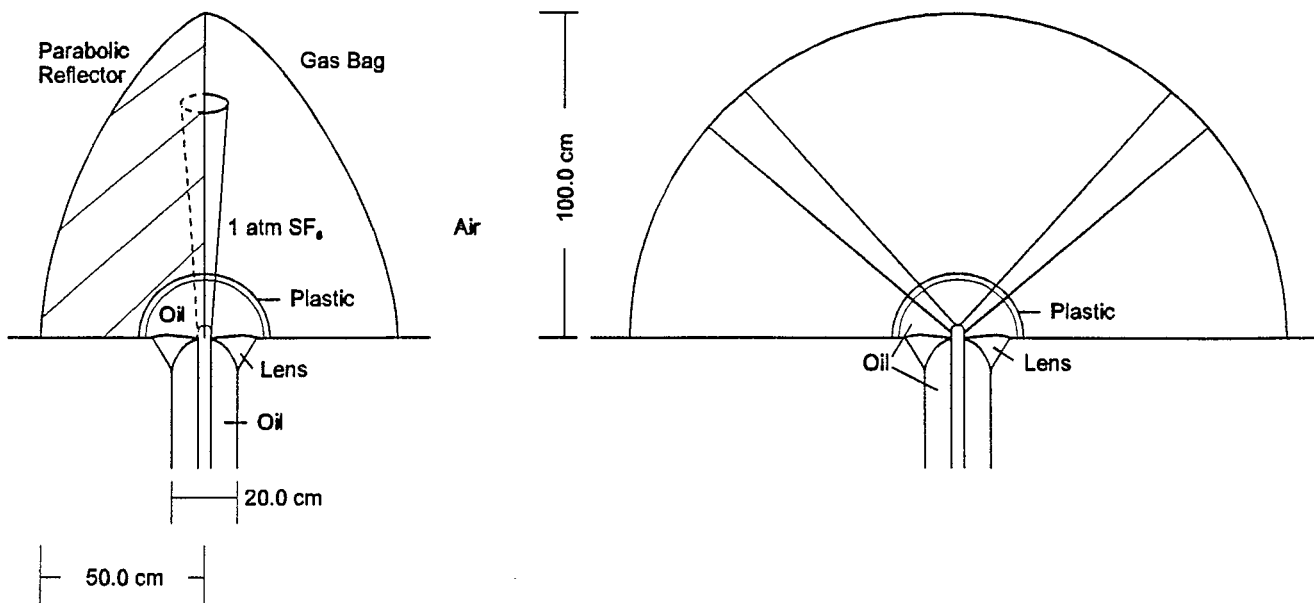


Figure 1.1 A sketch of the Half IRA, shown here with an oil cap.

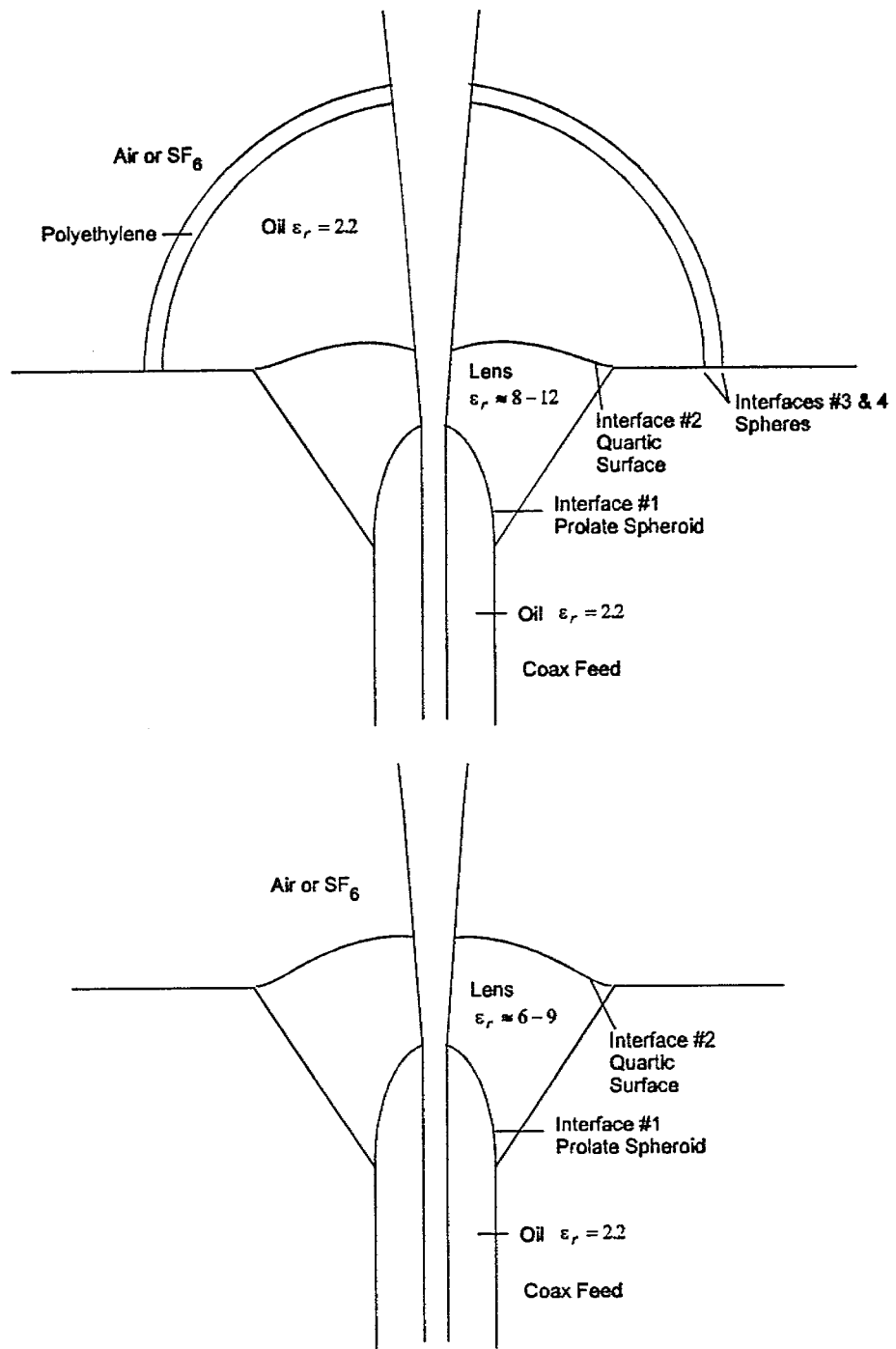


Figure 1.2. Two lens designs, including an oil cap (top) and without an oil cap (bottom).

II. Lens Equations

To design the lens, it is first necessary to derive the equations for the two interfaces, Interface #1 and Interface #2, as shown in Figure 1.2. The first interface is a simple prolate spheroid, and the second is a quartic surface, which is just a fourth-order polynomial. Although these were derived earlier in [4], we provide here derivations that are somewhat simpler for our special case.

A. Equations for the Interface #1: Plane Wave to Spherical Wave

The first interface converts an incident plane wave to a spherical wave. It is a prolate spheroid [4, Section 3], or ellipse of revolution. A diagram of the relevant parameters is shown in Figure 2.1. In the Ψ - z plane the equation of the surface is derived from transit-time considerations as

$$\sqrt{\epsilon_2}(\ell - r) = \sqrt{\epsilon_1}(-z) \quad (2.1)$$

This is just another way of saying that the ray through the center and an offset ray both must arrive at the circle at the same time. Let us make the substitution

$$q = \sqrt{\epsilon_1 / \epsilon_2} \quad , \quad q < 1 \quad (2.2)$$

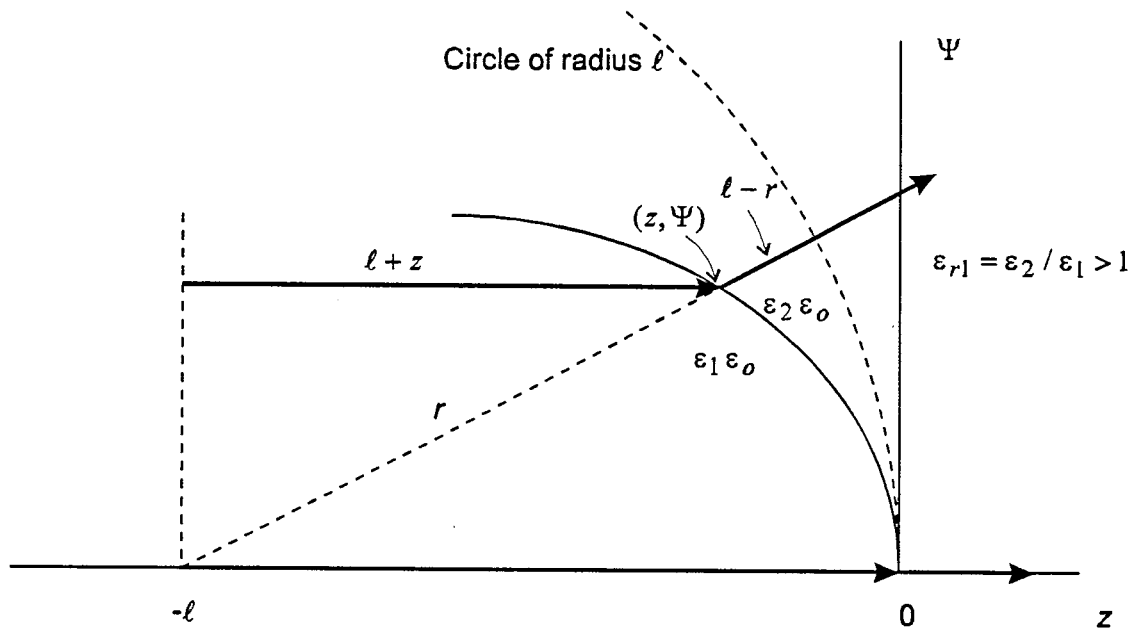


Figure 2.1. Geometry for Interface #1: Prolate spheroidal interface for converting a plane wave to a spherical wave.

In addition, we expand r into its z and Ψ components as

$$r^2 = (\ell + z)^2 + \Psi^2 \quad (2.3)$$

where Ψ is the radial cylindrical coordinate. (Note that Ψ is sometimes represented by other authors as ρ .) Combining the above three equations we find

$$(\ell + z)^2 + \Psi^2 = (\ell + qz)^2 \quad (2.4)$$

This is the equation to be solved.

By expanding and simplifying the above equation, we can find a simpler expression. After completing the square, we find

$$\begin{aligned} z^2 + \frac{2\ell}{1+q}z + \frac{\Psi^2}{1-q^2} &= 0 \\ \left(z + \frac{\ell}{1+q}\right)^2 + \frac{\Psi^2}{1-q^2} &= \frac{\ell^2}{(1+q)^2} \end{aligned} \quad (2.5)$$

If we now make the substitutions

$$a = \frac{\ell}{1+q}, \quad b = \ell \sqrt{\frac{1-q}{1+q}} \quad (2.6)$$

we arrive at the final equation

$$\frac{(z+a)^2}{a^2} + \frac{\Psi^2}{b^2} = 1 \quad (2.7)$$

This is immediately recognizable as a simple ellipse with major and minor axes of a and b , respectively, and offset in the z direction by $-a$. Note also that all rays in the second medium originate at one of the foci of the ellipse.

B. Equations for Interface #2: Spherical Wave to Another Spherical Wave

The second interface converts a spherical wave centered at $(-\ell_1, 0)$ to another spherical wave centered at $(-\ell_2, 0)$. A diagram of the rays to be traced is shown in Figure 2.2. Once again, from transit time considerations, we have

$$\sqrt{\varepsilon_2} r_1 + \sqrt{\varepsilon_3} (\ell_2 - r_2) = \sqrt{\varepsilon_2} \ell_1 \quad (2.8)$$

This was derived by enforcing the condition that a ray through the center and a ray through an off-center path must arrive at the circle at the same time. This simplifies further as

$$\begin{aligned}\sqrt{\epsilon_{r2}} (r_1 - l_1) &= (r_2 - l_2) \\ \epsilon_{r2} &= \epsilon_2 / \epsilon_3\end{aligned}\tag{2.9}$$

We can now expand r_1 and r_2 in terms of their z and Ψ components as

$$\begin{aligned}r_1 &= \sqrt{(\ell_1 + z)^2 + \Psi^2} \\ r_2 &= \sqrt{(\ell_2 + z)^2 + \Psi^2}\end{aligned}\tag{2.10}$$

Combining the above two equations, we now have the quartic equation that describes the surface,

$$\sqrt{\epsilon_{r2}} \left[\sqrt{(z + \ell_1)^2 + \Psi^2} - \ell_1 \right] = \left[\sqrt{(z + \ell_2)^2 + \Psi^2} - \ell_2 \right]\tag{2.11}$$

This corresponds to [4, equation 4.9]. To generate a curve from the above equation, we choose a set of Ψ values, and solve for z numerically. An explicit form of the surface is also available in [4].

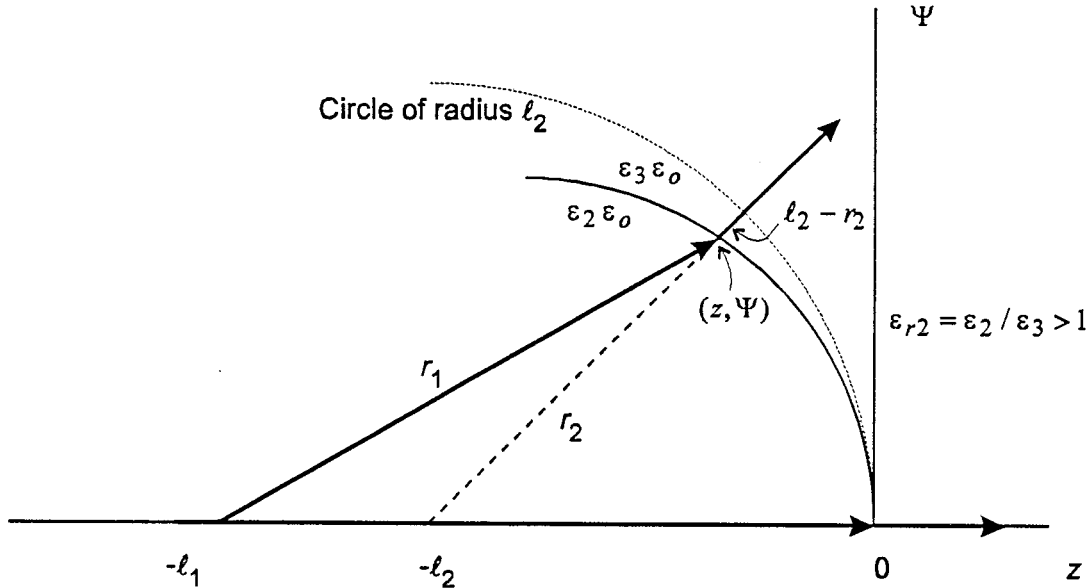


Figure 2.2. Geometry for Interface #2, a quartic surface for converting a spherical wave centered at $(-\ell_1, 0)$ to another spherical wave centered at $(-\ell_2, 0)$.

III. Lens Design Equations

We now begin the derivation of the overall lens equations. As a starting point, we express the equations of the two interfaces in a shifted coordinate system, as shown in Figure 3.1.

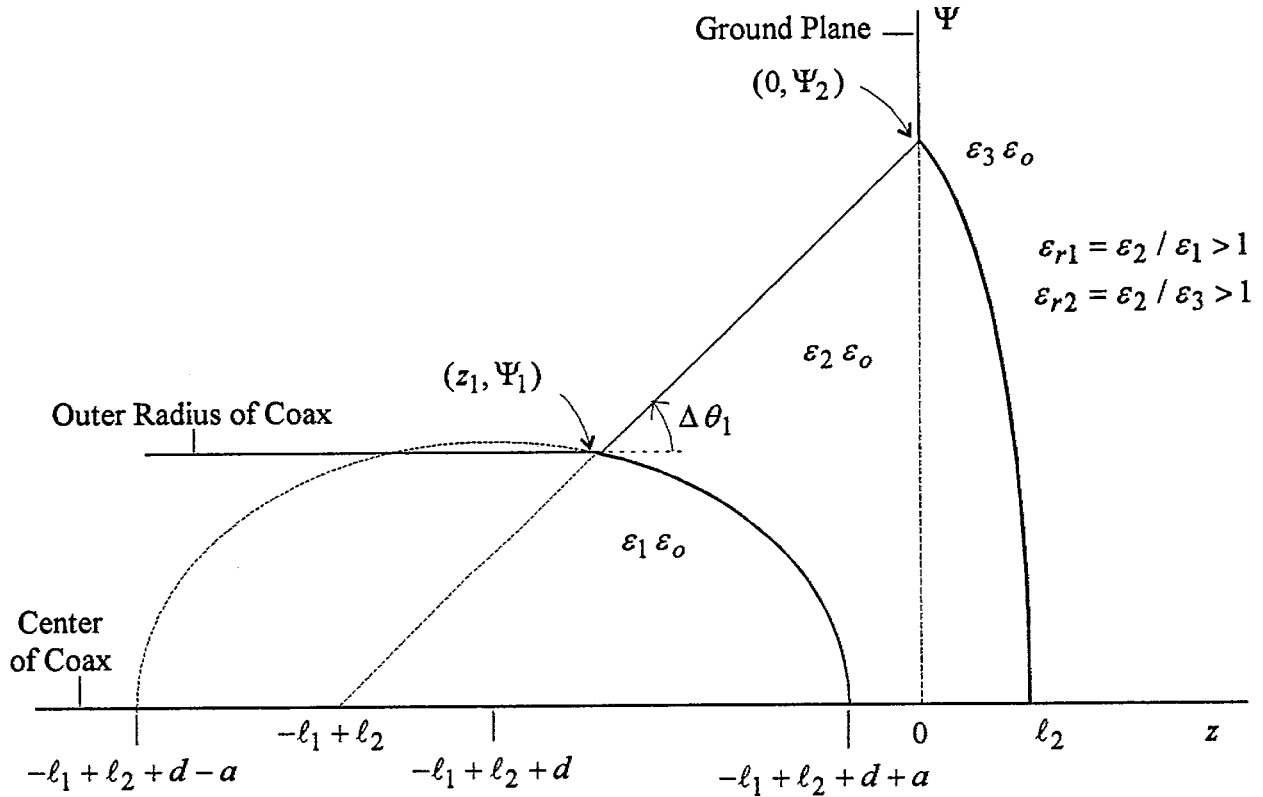


Figure 3.1. Lens design parameters.

The equations of the ellipse (prolate spheroid when rotated about the z axis) are

$$\frac{(z + l_1 - l_2 - d)^2}{a^2} + \frac{\Psi^2}{b^2} = 1 \quad (3.1)$$

$$d = \sqrt{a^2 - b^2}$$

Note that we use d to represent the focal distance instead of c , to avoid a conflict with the symbol for the speed of light. From (2.6) we know the dimensions of the ellipse are described by

$$b/a = \sqrt{1 - 1/\epsilon_{r1}}, \quad d/a = \frac{1}{\sqrt{\epsilon_{r1}}}, \quad \epsilon_{r1} = \epsilon_2 / \epsilon_1 \quad (3.2)$$

Furthermore, the equation for the quartic surface is

$$\begin{aligned}\sqrt{\varepsilon_{r2}} \sqrt{(z + \ell_1 - \ell_2)^2 + \Psi^2} - \sqrt{\varepsilon_{r2}} \ell_1 &= \sqrt{z^2 + \Psi^2} - \ell_2 \\ \varepsilon_{r2} &= \varepsilon_2 / \varepsilon_3\end{aligned}\tag{3.3}$$

This is our starting point in the procedure.

To design the lens, we choose ε_2 and $\Delta\theta_1$ as parameters. Typically we already know the relative dielectric constants ε_1 and ε_3 , because it has been decided in advance that oil will be at the input ($\varepsilon_1 = 2.2$) and either oil or air will be at the output ($\varepsilon_3 = 2.2$ or 1). Once these choices have been made, one can only adjust ε_2 and $\Delta\theta_1$. The dielectric constant of the lens is controlled by the choice of material from which it is machined. Thus, the design equations will be expressed in terms of ε_2 and $\Delta\theta_1$. We will also provide assistance in choosing these two parameters, and then solve some examples.

In fact, the solution process is a bit simpler if one chooses ε_2 and ℓ_2/ℓ_1 (instead of ε_2 and $\Delta\theta_1$) as parameters. We solved the problem this way originally, but we found more physical insight when $\Delta\theta_1$ is a parameter, because this is the angle the extreme ray is bent at Interface #1.

Finally, we note that the notation is a bit complicated, so we review the definitions of the dielectric constants. There are three relative dielectric constants, ε_1 , ε_2 , and ε_3 , representing the regions before, inside and after the lens, respectively. In addition, since all of our equations are dependent only upon a ratio of dielectric constants between adjoining regions, we have defined two dielectric constant ratios as

$$\begin{aligned}\varepsilon_{r1} &= \varepsilon_2 / \varepsilon_1 , & \varepsilon_{r1} &> 1 \\ \varepsilon_{r2} &= \varepsilon_2 / \varepsilon_3 , & \varepsilon_{r2} &> 1\end{aligned}\tag{3.4}$$

These can easily be remembered if one recalls that ε_2 is the highest dielectric constant of the three, and each of our dielectric constant ratios is just the ratio of the high dielectric constant to the low dielectric constant at the first and second interface.

A. Design of Interface #1

The first step in the analysis is to find Ψ_1 , as shown in Figure 3.1, based on dielectric breakdown considerations. In a typical problem, one might have to allow the coax to be large enough to carry a certain peak power, without exceeding some limit on the electric field on the center conductor. The procedure for doing so has already been described in [5].

Next, we have to find a/Ψ_1 for the given parameters of ε_{r1} and $\Delta\theta_1$. Starting from (3.1), we substitute $(z, \Psi) = (z_1, \Psi_1)$ and rearrange to find

$$\begin{aligned}\cot(\Delta\theta_1) &= \frac{z_1 + \ell_1 - \ell_2}{\Psi_1} = \frac{a}{\Psi_1} \sqrt{1 - \left(\frac{\Psi_1}{b}\right)^2} + \frac{d}{\Psi_1} \\ &= \sqrt{\left(\frac{a}{\Psi_1}\right)^2 - \left(\frac{a}{b}\right)^2} + \frac{a}{\Psi_1} \sqrt{1 - \left(\frac{b}{a}\right)^2}\end{aligned}\quad (3.5)$$

where we have used $d = \sqrt{a^2 - b^2}$ in the final step. Substituting the value of b/a from (3.2), we have

$$\cot(\Delta\theta_1) = \sqrt{\left(\frac{a}{\Psi_1}\right)^2 - \frac{\epsilon_{r1}}{\epsilon_{r1} - 1}} + \frac{a}{\Psi_1} \frac{1}{\sqrt{\epsilon_{r1}}}\quad (3.6)$$

Next, we shift the final term on the right to the left side, and square both sides. After simplifying, we find

$$\left(\frac{a}{\Psi_1}\right)^2 + \frac{2\sqrt{\epsilon_{r1}}}{\epsilon_{r1} - 1} \cot(\Delta\theta_1) \left(\frac{a}{\Psi_1}\right) - \left[\frac{\epsilon_{r1}^2}{(\epsilon_{r1} - 1)^2} + \frac{\epsilon_{r1}}{\epsilon_{r1} - 1} \cot^2(\Delta\theta_1)\right] = 0\quad (3.7)$$

This can be solved for (a/Ψ_1) since it is just a quadratic equation. After doing so, and after applying the trigonometric identity $\cot^2(\theta) + 1 = \csc^2(\theta)$, the result simplifies to

$$\frac{a}{\Psi_1} = \frac{\sqrt{\epsilon_{r1}}}{\epsilon_{r1} - 1} \left[\sqrt{\epsilon_{r1}} \csc(\Delta\theta_1) - \cot(\Delta\theta_1) \right]\quad (3.8)$$

This is the result we needed. Since Ψ_1 has already been determined, one can find a from (3.8), and b and d from (3.2). Note that the solution to the quadratic equation actually generates a solution with a “ \pm ” sign in front of the cosecant term above. But the minus sign makes no physical sense, because a/Ψ_1 cannot be negative.

At this point, the absolute size and shape of the ellipse is defined, but its location on the z axis is still unknown. For this, we need to solve the quartic equation.

B. Design of Interface #2

The ultimate goal in the design of the quartic surface is to calculate ℓ_2/ℓ_1 , or equivalently ℓ_1/ℓ_2 . To do so, we begin by substituting $(z, \Psi) = (0, \Psi_2)$ into the quartic equation, (3.3). After dividing both sides by ℓ_1 , we find

$$\sqrt{\varepsilon_{r2}} \sqrt{\left(1 - \frac{\ell_2}{\ell_1}\right)^2 + \left(\frac{\Psi_2}{\ell_1}\right)^2} - \sqrt{\varepsilon_{r2}} = \frac{\Psi_2}{\ell_1} - \frac{\ell_2}{\ell_1} \quad (3.9)$$

We now need to solve for Ψ_2/ℓ_1 . To do so, we shift the second term on the left side to the right side, and square both sides. After much rearranging, and after solving a quadratic equation, we find

$$\frac{\Psi_2}{\ell_1} = \frac{-\frac{\ell_2}{\ell_1} + \sqrt{\varepsilon_{r2}} + \sqrt{\varepsilon_{r2}} \sqrt{(2 - \varepsilon_{r2}) \left(\frac{\ell_2}{\ell_1}\right)^2 + 2(\varepsilon_{r2} - \sqrt{\varepsilon_{r2}} - 1) \left(\frac{\ell_2}{\ell_1}\right) + 1}}{\varepsilon_{r2} - 1} \quad (3.10)$$

We now need to get Ψ_2/ℓ_1 into a form that is related to $\Delta\theta_1$. To do so, we know

$$\cot(\Delta\theta_1) = \frac{\ell_1 - \ell_2}{\Psi_2} = \frac{1 - (\ell_2/\ell_1)}{\Psi_2/\ell_1} \quad (3.11)$$

Combining the above two equations, we find

$$\cot(\Delta\theta_1) = \frac{(\varepsilon_{r2} - 1) \left(1 - \frac{\ell_2}{\ell_1}\right)}{-\frac{\ell_2}{\ell_1} + \sqrt{\varepsilon_{r2}} + \sqrt{\varepsilon_{r2}} \sqrt{(2 - \varepsilon_{r2}) \left(\frac{\ell_2}{\ell_1}\right)^2 + 2(\varepsilon_{r2} - \sqrt{\varepsilon_{r2}} - 1) \left(\frac{\ell_2}{\ell_1}\right) + 1}} \quad (3.12)$$

The only unknown in this equation is ℓ_2/ℓ_1 . The simplest method to obtain it is to solve the above equation numerically for ℓ_2/ℓ_1 . For the cases we tried, convergence was easily obtained starting from any reasonable initial guess. It is, however, possible to solve this equation analytically. After a bit of work, we find

$$\frac{\ell_2}{\ell_1} = \frac{\sqrt{\varepsilon_{r2}} (\sqrt{\varepsilon_{r2}} - 1) \cot^2(\Delta\theta_1) [1 - \sec(\Delta\theta_1)] - (\sqrt{\varepsilon_{r2}} + 1) \cot(\Delta\theta_1) + (\varepsilon_{r2} - 1)}{(\varepsilon_{r2} - 1) \csc^2(\Delta\theta_1) - 2 \cot(\Delta\theta_1)} \quad (3.13)$$

Note that the term in square brackets above is actually found to be $[1 \pm \sec(\Delta\theta_1)]$, which comes from two solutions to a quadratic equation. By experimenting with both signs, and after comparing to the numerical solution of (3.12), we find the minus sign is correct.

All that is left is to specify Ψ_2 , and it turns out that there is some flexibility in choosing this parameter. The only restriction is that it must be large enough so that the two interfaces do not intersect near the center. To enforce this, we see by inspecting Figure 3.1 that

$$\begin{aligned} \ell_1 &\geq a + d \\ \frac{\ell_1}{\Psi_2} &\geq \left(1 + \frac{d}{a}\right) \left(\frac{a}{\Psi_1}\right) \left(\frac{\Psi_1}{\Psi_2}\right) \end{aligned} \quad (3.14)$$

Now, using the fact that $d/a = 1/\sqrt{\varepsilon_{r1}}$, we rearrange to find a lower bound on Ψ_2 of

$$\Psi_2 \geq \Psi_1 \left(1 + \frac{1}{\sqrt{\varepsilon_{r1}}}\right) \left(\frac{a}{\Psi_1}\right) \left(\frac{\Psi_2}{\ell_1}\right) \quad (3.15)$$

where a/Ψ_1 is provided in (3.8) and Ψ_2/ℓ_1 is provided in (3.10). This is alternatively expressed as

$$\begin{aligned} \Psi_2 &\geq \Psi_{2\min} \\ \Psi_{2\min} &= \Psi_1 \left(1 + \frac{1}{\sqrt{\varepsilon_{r1}}}\right) \left(\frac{a}{\Psi_1}\right) \left(\frac{\Psi_2}{\ell_1}\right) \end{aligned} \quad (3.16)$$

Thus, any value of Ψ_2 greater than $\Psi_{2\min}$ is acceptable. Note that a slightly smaller Ψ_2 will be acceptable if there is a center conductor, because the two interfaces first touch at the center conductor.

Since we now have a value for Ψ_2 , we can use (3.10), to solve for Ψ_2/ℓ_1 . This leads to ℓ_1 , and since ℓ_1/ℓ_2 is known, we have ℓ_2 as well. Thus, the entire problem is solved, for the given set of parameters ε_2 and $\Delta\theta_1$, and assuming ε_1 and ε_3 are already chosen. In the section that follows, we provide assistance in choosing ε_2 and $\Delta\theta_1$.

IV. Limits on $\Delta\theta_1$

Having calculated the two surfaces in terms of the dielectric constants and $\Delta\theta_1$, we now explore how to choose these values intelligently. Assuming that ε_1 and ε_3 are already chosen, then for a given ε_2 , one can identify both maximum and minimum limits on the values of $\Delta\theta_1$. In addition, one can rule out values of ε_2 below a minimum value, because no solution is possible there.

A. Maximum $\Delta\theta_1$ Based on Grazing Incidence at Interface #1

Let us consider the maximum possible bend at Interface #1 for a given $\varepsilon_{r1} = \varepsilon_2/\varepsilon_1$. Theoretically, one can bend the extreme ray by the greatest angle if it is incident at grazing angle, or $\theta_{i1} = 90^\circ$. Of course, this is not a good choice, because the E-field transmission coefficient is zero there. But it does place an absolute limit on how large $\Delta\theta_1$ can be. For this case, the transmitted angle is

$$\theta_{t1} = \arcsin(1/\sqrt{\varepsilon_{r1}}) \quad (4.1)$$

So the maximum bend one can achieve at Interface #1 is

$$\Delta\theta_{1Max} = 90^\circ - \arcsin(1/\sqrt{\varepsilon_{r1}}) \quad (4.2)$$

For a given $\varepsilon_{r1} = \varepsilon_2/\varepsilon_1$, this limits the choice of $\Delta\theta_1$. We will plot this function later, when we also have a minimum value of $\Delta\theta_1$. Because we assume here grazing incidence, this is a loose upper bound, and one must avoid it in practice.

B. Minimum $\Delta\theta_1$ Based on $\ell_2/\ell_1 = 0$ in the Quartic Equation

If one experiments with the quartic equation a bit, one sees readily that it is difficult to decrease $\Delta\theta_1$ as much as one would like. For a given $\varepsilon_{r2} = \varepsilon_2/\varepsilon_3$, one obtains the minimum $\Delta\theta_1$ in the limit as $\ell_2/\ell_1 \rightarrow 0$. One can then calculate the resulting $\Delta\theta_1$ with the understanding that this is the maximum achievable for a given ε_{r2} .

To see the effect, we substitute $(z, \Psi) = (0, \Psi_2)$ into the quartic equation, (3.3). We then take the limit as $\ell_2/\ell_1 \rightarrow 0$ by substituting $\ell_2 = 0$. From this we find

$$\sqrt{\varepsilon_{r2}} \sqrt{\ell_1^2 + \Psi_2^2} - \sqrt{\varepsilon_{r2}} \ell_1 = \Psi_2 \quad (4.3)$$

We move the second term to the right hand side, square both sides and simplify, to find

$$\frac{\Psi_2}{\ell_1} = \frac{2\sqrt{\varepsilon_{r2}}}{\varepsilon_{r2} - 1} \quad (4.4)$$

Now, $\Delta\theta_1$ is determined from

$$\cot(\Delta\theta_{1Min}) = \frac{\ell_1 - \ell_2}{\Psi_2} \Big|_{\ell_2=0} \quad (4.5)$$

Combining the above two equations, we have a minimum $\Delta\theta_1$ of

$$\Delta\theta_{1Min} = \text{arccot} \left(\frac{\epsilon_{r2} - 1}{2\sqrt{\epsilon_{r2}}} \right) \quad (4.6)$$

We now have minimum and maximum values for $\Delta\theta_1$ as a function of ϵ_2 .

We can plot the minimum and maximum values of $\Delta\theta_1$ as a function of ϵ_2 for two specific cases. The two cases we consider are the oil-lens-oil design and the oil-lens-air design, and the results are shown in Figure 4.1. In both designs, there is a crossover, below which no solution is possible. For the oil-air-oil design, the crossover occurs at $\epsilon_2 = 7.44$, and for the oil-lens-air design this occurs at $\epsilon_2 = 4.97$. Below the crossover values, the lens has a dielectric constant too low to bend the rays sufficiently. Thus, to allow some design flexibility, one will want to use somewhat higher values of ϵ_r than the minimum values.

Note that there appears to be no particular penalty for being too close to the minimum value of $\Delta\theta_1$, for a given ϵ_2 . In this case, ℓ_2/ℓ_1 is zero, but that does not affect lens performance. In fact, imposing $\ell_2/\ell_1 = 0$ may have some advantage, if one wants to keep the lens thin at its center. This can happen if one wants to keep the feed arm attachment outside the lens. On the other hand, having a $\Delta\theta_1$ near the maximum implies grazing incidence for the extreme ray at Interface #1. Thus, the maximum value of $\Delta\theta_1$ must be avoided. This implies that one must use an ϵ_2 somewhat higher than the crossover value.

When comparing the two plots, we find that the oil-lens-air design has a lower crossover than the oil-lens-oil design. This implies that a lower dielectric constant can be used for the lens. This is an advantage, because a lower dielectric constant leads to less reflection loss.

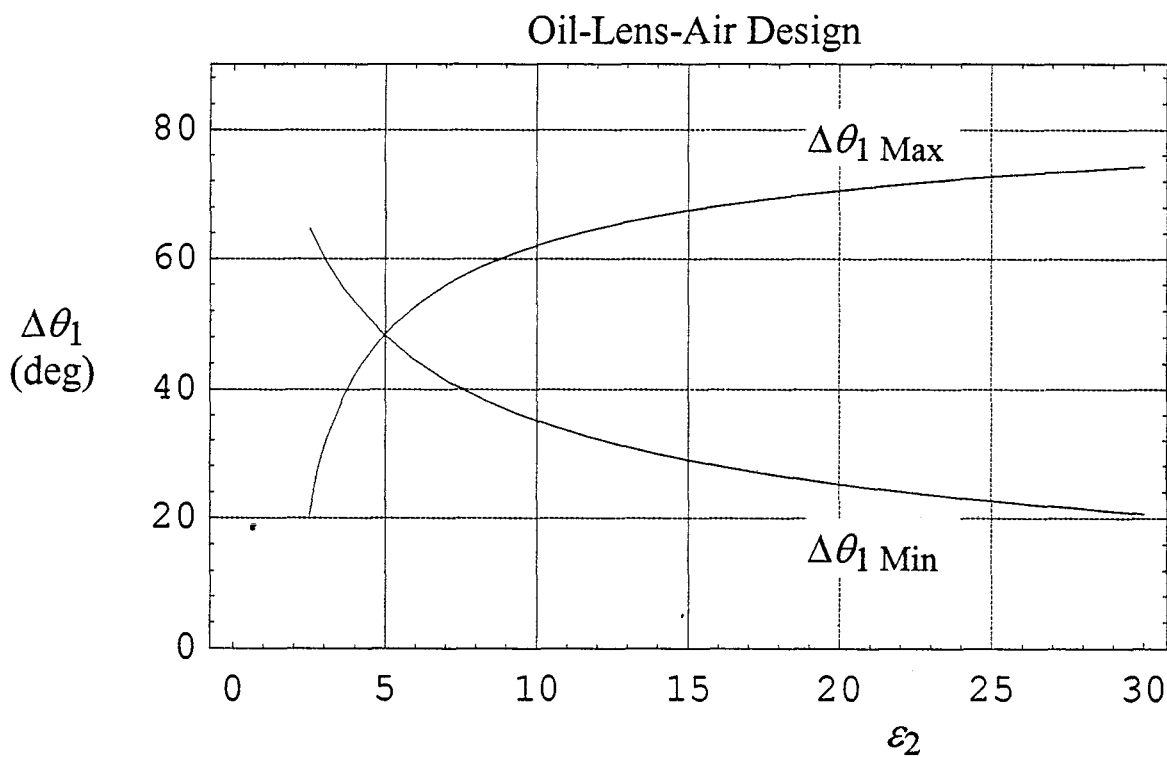
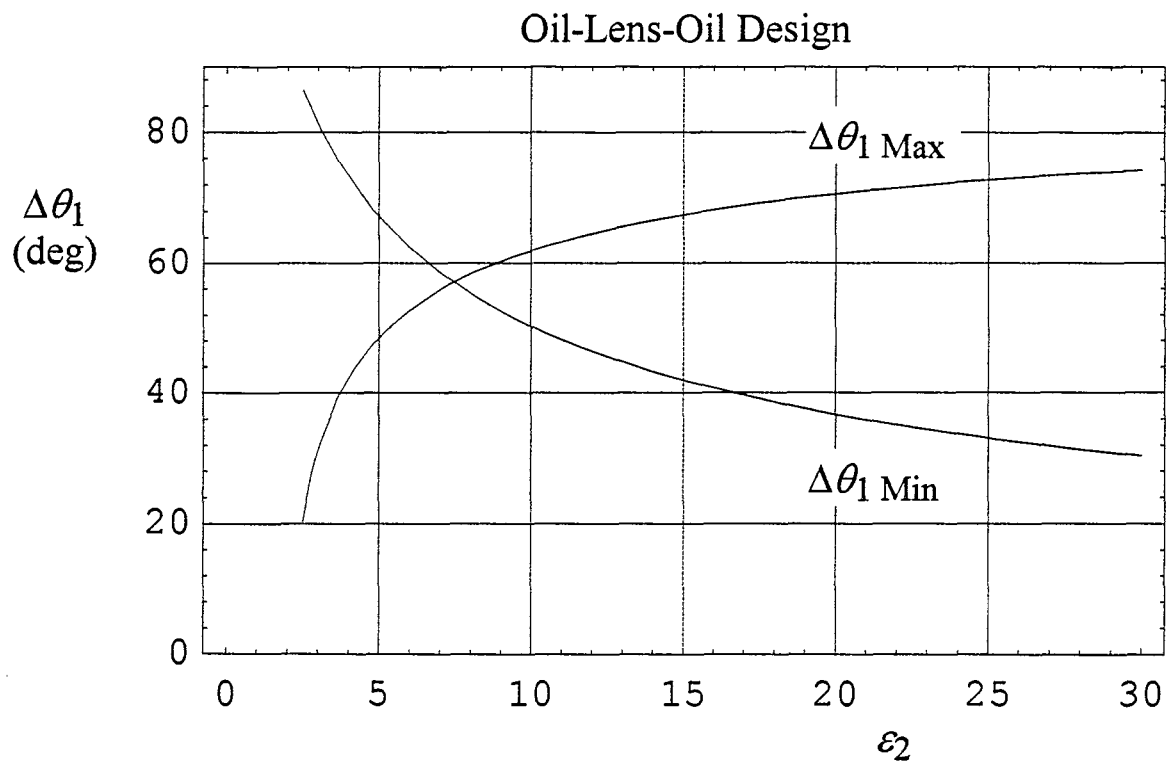


Figure 4.1. Minimum and maximum values of $\Delta\theta_1$ for the oil-lens-oil case (top) and the oil-lens-air case (bottom). Oil is assumed to have a dielectric constant of 2.2.

V. Some Examples

Let us now consider an example in which an oil-filled coaxial structure is used to feed a 100 Ω HIRA, with a lens of dielectric constant 11. A further assumption is that one can sustain a peak electric field in oil of 1 MV/cm on the center conductor without breakdown (approximately valid for pulses ~ 1 ns in duration). We calculate the lens shape for two different configurations, an oil-lens-oil configuration and an oil-lens-air configuration.

First, we calculate the parameters for the feed line, which is shown in Figure 5.1. Since the antenna impedance in air is 100 Ω , the impedance of the coaxial feed in oil is 67 Ω , assuming the conductors are continuous at the interface. We find the peak voltage using

$$V_{\max} = \sqrt{Z_c P_{\max}} \quad (5.1)$$

and we find a maximum voltage of 2.6 MV. To find the outer radius, we use [5, eqn. 4.5]

$$\begin{aligned} E_{\max} &= E_{\text{norm}} \frac{V}{\Psi_1} \\ E_{\text{norm}} &= \frac{e^{2\pi f_g \sqrt{\epsilon_1}}}{2\pi f_g \sqrt{\epsilon_1}} \end{aligned} \quad (5.2)$$

where $f_g = Z_c/(376.727 \Omega)$ and Ψ_1 is the outer radius, so E_{norm} is found to 3.2 at 67 Ω . Assuming a maximum electric field in oil of $E_{\max} = 1$ MV/cm, we then find an outer radius of 8.3 cm. Finally, the radius of the center conductor is calculated from

$$\frac{\Psi_1}{\Psi_o} = e^{2\pi f_g \sqrt{\epsilon_1}} \quad (5.3)$$

where Ψ_o is the inner radius. Thus, for $f_g = 67/377$ and $\epsilon_1 = 2.2$, we have $\Psi_1/\Psi_o = 5.2$. Thus, a reasonable feed geometry is $\Psi_1 = 8.5$ cm and $\Psi_o = 1.62$ cm, for the inner and outer conductors, respectively.

Next, we choose the lens dielectric constant and $\Delta\theta_1$ in a manner consistent with the known limitations. We would like to choose values that will work with both the oil-lens-oil and the oil-lens-air configurations. After consulting Figure 4.1, it is found that the values of $\epsilon_2 = 11$ and $\Delta\theta_1 = 50^\circ$ are consistent with the known limitations for both cases, so we use these values.

Now, we solve the oil-lens-oil configuration. From (3.8) we find $a/\Psi_1 = 1.16$, so $a = 9.88$ cm. From (3.2) we find $b = 8.84$ cm and $d = 4.42$ cm. From (3.13) we find $\ell_1/\ell_2 = 25.29$. Next, we find from (3.16) the minimum value of Ψ_2 is 16.37 cm, so we choose $\Psi_2 = 17$ cm, for which $\Psi_2/\Psi_1 = 2.0$. From (3.10) we have $\Psi_2/\ell_1 = 1.145$, so $\ell_1 = 14.85$ cm and $\ell_2 = 0.59$ cm. Using these values, we have plotted the complete lens on the top in Figure 5.2.

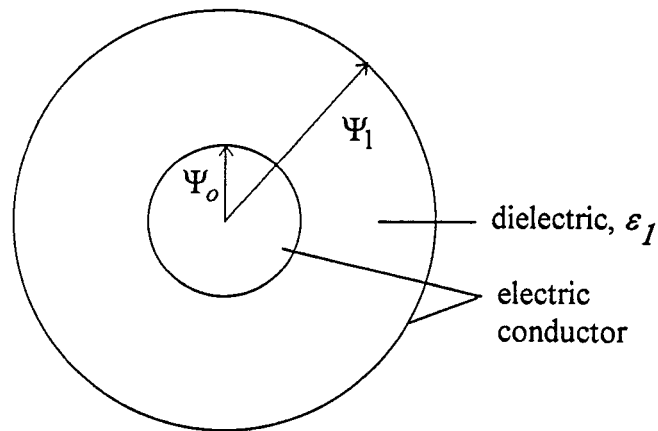


Figure 5.1. A coaxial geometry.

Next, we repeat the process with the oil-lens-air design. The dimensions of the resulting ellipse are the same as before, i.e., $a = 9.88$ cm, $b = 8.84$ cm and $d = 4.42$ cm. Furthermore, we find $\ell_1/\ell_2 = 4.56$, and the minimum value of Ψ_2 is 13.30 cm. Once again, we choose $\Psi_2 = 17$ cm, for which $\Psi_2/\Psi_1 = 2.0$. Finally, we have $\Psi_2/\ell_1 = 0.930$, so $\ell_1 = 18.28$ cm and $\ell_2 = 4.01$ cm. Using these values, we have plotted the complete lens on the bottom in Figure 5.2.

It is interesting to compare the two resulting lenses. In fact, they are quite similar in shape, except that when air is used at the output, the lens is fatter in the center.

Note that we have chosen the values of ϵ_2 and $\Delta\theta_1$ somewhat arbitrarily. In the case of the oil-lens-air design, one can use a considerably lower lens dielectric constant, which reduces reflections. An example of a better lens design is shown in Figure 5.3. We use here a lens dielectric constant of 6.6 and air (or SF_6) at the output. For this design, $\Delta\theta_1 = 43^\circ$, $a = 10.80$ cm, $b = 8.82$ cm and $d = 6.24$ cm. Furthermore, we find $\ell_1/\ell_2 = 141.5$, and the minimum value of Ψ_2 is 15.77 cm. Again, we choose $\Psi_2 = 17$ cm, for which $\Psi_2/\Psi_1 = 2.0$. Finally, we have $\Psi_2/\ell_1 = 0.9259$, so $\ell_1 = 17.44$ cm and $\ell_2 = 0.123$ cm.

The improved design has a number of advantages over the first two designs, besides reduced reflections. The lens is thin at its center, so we can easily build a center conductor that splits into two feed arms just after the lens. If the lens is too thick, the split is too far to the right of $z = 0$, thus destroying the conical symmetry. Another advantage is that no oil cap is required, thus reducing feed blockage. A possible disadvantage is that there is less dielectric strength at the output without an oil cap. But if the duration of the pulse is short enough, there will be insufficient time for the pulse to cross the large gap (~ 15 cm) from the center conductor to the ground plane.

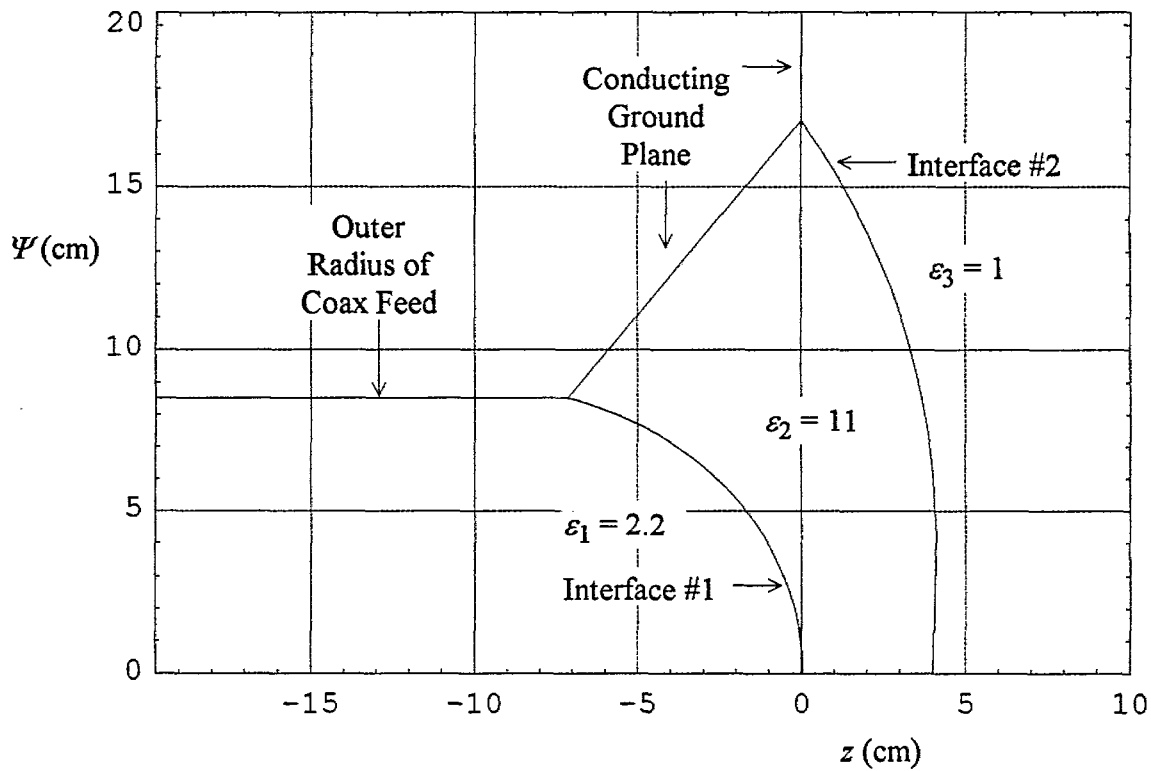
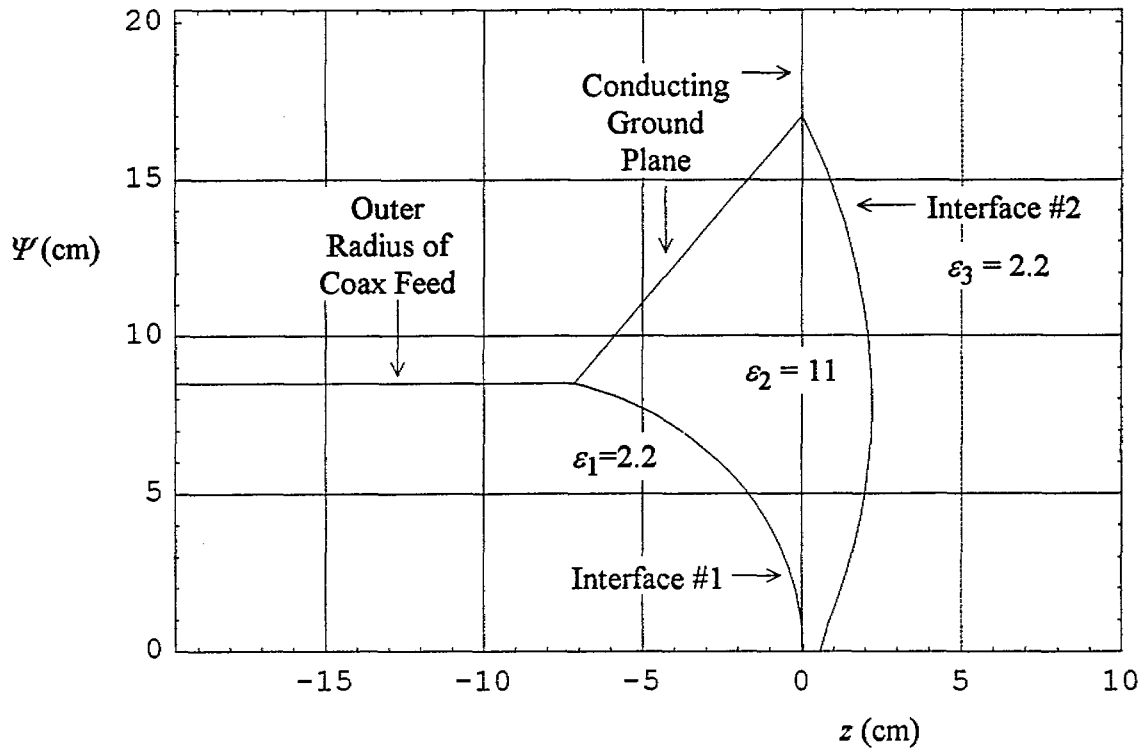


Figure 5.2. Lens design for the oil-lens-oil case (top) and the oil-lens-air case (bottom), with $\Delta\theta_1 = 50^\circ$, and $\Psi_2/\Psi_1 = 2$.

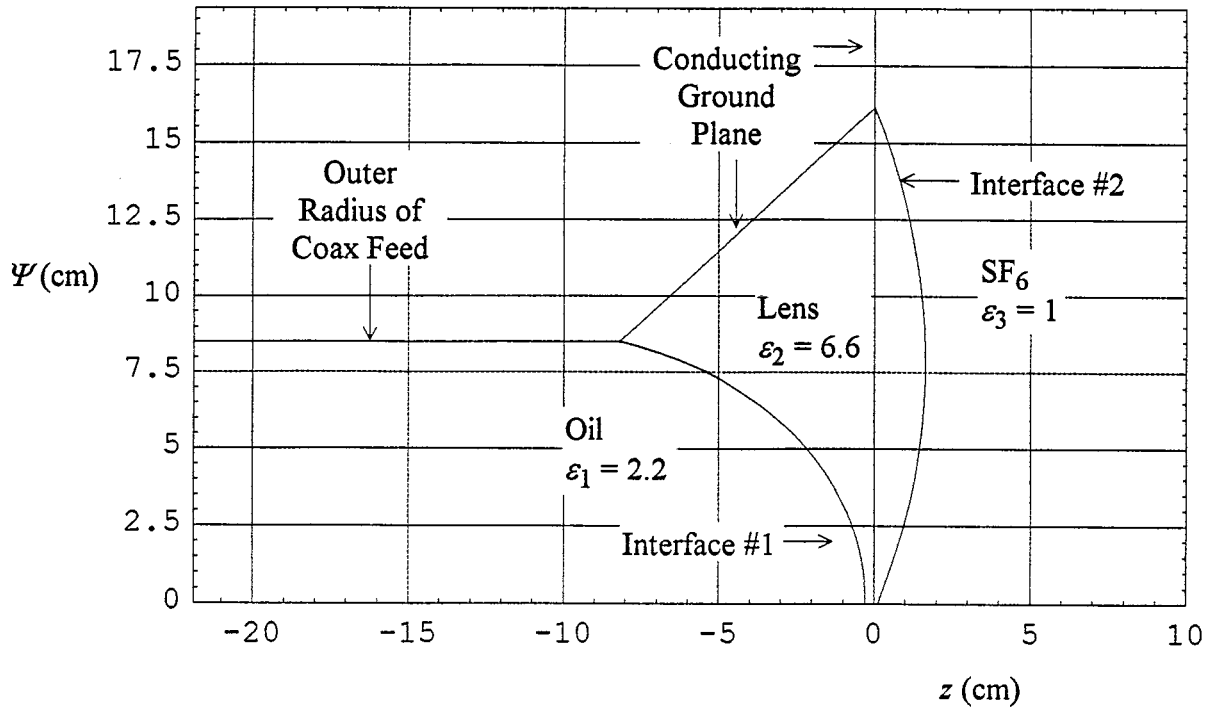


Figure 5.3. Improved oil-lens-air design using $\Delta\theta_1 = 43^\circ$, and $\Psi_2/\Psi_1 = 2$.

VI. Concluding Remarks

We have provided here the design equations and some sample designs for the feed-point lens needed to build a high-voltage half IRA. Although we have demonstrated solutions to the equations, we have not yet attempted to optimize the lens to achieve a maximum transmission coefficient. That is, we have chosen the dielectric constants and $\Delta\theta_1$ somewhat arbitrarily. In a later paper we hope to solve the optimization problem.

Acknowledgments

We would like to thank Mr. William D. Prather of Phillips Laboratory for funding portions of this work. We would also like to thank Dr. Gary D. Sower for many helpful discussions relating to this work.

References

1. C. E. Baum, Variations on the Impulse-Radiating Antenna Theme, Sensor and Simulation Note 378, February 1995.
2. E. G. Farr and C. E. Baum, Impulse Radiating Antennas With Two Reflecting or Refracting Surfaces, Sensor and Simulation Note 379, May 1995.
3. C. E. Baum and A. P. Stone, *Transient Lens Synthesis: Differential Geometry in Electromagnetic Theory*, Appendix I, Taylor and Francis, New York, 1991.
4. C. E. Baum, J. J. Sadler, and A. P. Stone, Uniform Isotropic Dielectric Equal-Time Lenses for Matching Combinations of Plane and Spherical Waves, Sensor and Simulation Note 352, December 1992.
5. E. G. Farr, et al, Design Considerations for Ultra-Wideband, High-Voltage Baluns, Sensor and Simulation Note 371, October 1994.